

Utility of Earth Observation data in mapping post-disaster impact: A case of Hurricane Dorian in the Bahamas

Mohammed Ozigis^a, Oluropo Ogundipe^b, Samuel J. Valman^c, Jessica L. Decker Sparks^d, Helen McCabe^e, Rebekah Yore^f, Bethany Jackson^{g,*}

^a Biology and Environmental Science, Liverpool John Moores University, Liverpool, UK

^b Global Geo-Intelligence Solutions Ltd., Nottingham, UK

^c School of Geography and Nottingham Geospatial Institute, University of Nottingham, Nottingham, UK

^d Friedman School of Nutrition Science and Policy, Tufts University, Boston MA, USA

^e School of Politics and International Relations and Rights Lab, University of Nottingham, Nottingham, UK

^f Rescue Global, London, UK and Institute for Risk and Disaster Reduction, University College London, London, UK

^g School of Geography and Rights Lab, University of Nottingham, Nottingham, UK

1. Introduction

As a low-lying island state, the geography of The Bahamas makes it vulnerable to disasters resulting from hurricanes (Schultz et al., 2020) that are increasing in intensity and strength as the world experiences anthropogenic climate change related impacts (Reed et al., 2022). Structural inequalities, such as poverty, racial and gender discrimination, and migration status, can be exacerbated by climate change impacts, sometimes increasing vulnerability to human trafficking and exploitation (Bharadwaj et al., 2021).

Earth Observation (EO) has a history of applied data to support areas that have experienced environmental hazards, including real-time monitoring of events (assessing the scale, scope and duration) and following the aftermath of impacts to support on-ground support provisions (USAID, 1991). The role of EO in this capacity has been strengthened by the establishment of the International Charter Program (Stryker and Jones, 2009) with data being gathered from multiple satellites (Percivall et al., 2013; Vongsantivanich et al., 2018) during hazard responses. EO applications during the response phase of crises are most noted (Boccardo and Tonolo, 2015; Voigt et al., 2007), although prevention and preparedness are increasingly supported (Le Cozannet et al., 2020; Nhamo and Chikodzi, 2021). Satellite monitoring following hazards has been applied to earthquakes, volcanic eruptions, flooding and landslides, and coastal hazards such as storm surges and tsunamis (Tralli et al., 2005).

Beyond hazard response, EO data has also been applied to investigate and support in-country responses to social challenges noted in the UN Sustainable Development Goals (SDGs). For example, several studies that have sought to investigate literacy rates (Watmough et al., 2013), as well as health outcomes (Patz, 2005; Sorek-Hamer et al., 2016; Head et al., 2017) and poverty rates (Elvidge et al., 2012; Blumenstock, 2016; Bennett and Smith, 2017; Hargreaves and Watmough, 2020). Moreover, work has been undertaken to explore the application of EO data to support ground-based action on issues of forced labour in industries such as brick manufacturing (Boyd et al., 2018, 2021; Foody et al., 2019), forestry (Jackson et al., 2020a), fishing (Jackson et al., 2020b), agriculture (Koukoulou et al., 2021), and mining (Brownet et al., 2020, 2022). Disaster events have been noted as key risk to increasing the vulnerability of communities and their exposure to human trafficking risks when responding to hazards such as hurricanes (Bales, 2021). Heightened risks to human trafficking in the same region as The Bahamas have been noted following events such as Hurricane Katrina (Stout, 2018;

* Corresponding author.

E-mail address: bethany.jackson1@nottingham.ac.uk (B. Jackson).

Bales, 2021) linked to poor responses. This builds upon the interconnected risks of human trafficking and climate change, where communities can be exposed to factors that may lead to human trafficking (Coelho, 2016). As such, applying satellite EO data to assess both hazards and social risks provides a unique opportunity to understand increased community vulnerabilities, for example, marginalisation of communities following hazard events and potential exposure to human trafficking risks. Previous post-disaster mapping assessments have used a variety of index measures including vegetation assessments, building damage measures, and innovations including SAR indices and machine learning approaches (e.g., Hoque et al., 2017; Ghaffarian et al., 2020; Karaer et al., 2021; Deng and Wang, 2022; Li et al., 2023; Al Shafian and Hu, 2024). However, none have targeted those seeking to support populations who may be vulnerable to the risks of exploitation following a hazard impact – thus this paper targets an audience that has largely been overlooked. Further, the paper builds on the identified niche themes for applications of satellite imagery assessment to support emergency response (Greenal and Anilkumar 2024) with a targeted population (those vulnerable to trafficking) in mind.

Hurricane Dorian is an interesting case study for the various social-ecological impacts experienced by communities. The storm (a Category 5) struck The Bahamas in September 2019, making landfall on the northwestern island of Abaco before lingering over Grand Bahama (see Fig. S1). Dorian struck the islands for three days due to weakening pressure and the collapse of the steering currents making it the strongest hurricane to hit The Bahamas in modern history (Avila et al., 2020). The hurricane caused an estimated US\$3.4 billion in damage and losses (Zegarra et al., 2020). Nearly 10,000 people were displaced (Marazita, 2020) and official deaths were reported for 74 people with a further 282 officially still missing (IFRC, 2023). Some of the official figures are likely to be an undercount because many from the Haitian diaspora were severely impacted; and the political and cultural discrimination against the Haitian community in The Bahamas is likely to have led to an underreporting of the impact of Hurricane Dorian upon this community (Thomas and Benjamin, 2022; Smith, 2019; Behm, 2019). The impact of the storm has since been compounded by the Covid-19 pandemic (Bethell-Bennett et al., 2022) which has significantly affected recovery efforts.

Building on the application of satellite data to assess risks post-hurricane in other Caribbean contexts (e.g., Hurricanes Maria and Irma, on the island of Puerto Rico; de Beurs et al., 2019; Marlier et al., 2022; Zegarra et al. (2020) provided detailed tracking and assessment of overall economic losses resulting from Hurricane Dorian; and immediate visible changes using optical sensors were identified (Inter-American Development Bank, 2020). Beyond the overall descriptive assessments, there has been a focus on the scale of vegetation losses (McKenzie et al., 2023) using optical data. Further, synthetic aperture radar (SAR) data from Sentinel-1 were used to evaluate the extent of flooding in The Bahamas (Cerrai et al., 2020). Some efforts have been made to integrate EO data with social information to assess the risks of floods and generate mapping (Sadiq et al., 2022). Other sources of EO data have also been applied. For example, unmanned aerial vehicle (UAV) data were used to understand the scale of infrastructure damage (Cheng et al., 2021). Night-light data were also used by Zegarra et al. (2021) to assess the economic impact and losses across the archipelago.

In this study, we assessed the impact of Hurricane Dorian by conducting a pre-, during- and post-hurricane analysis, combining optical and radar data, applying a series of indices to identify the most influential environmental factors which expose populations in The Bahamas to hazards and potentially human trafficking risks based on Earth Observation (EO) analyses. We evaluated the ability to assess changes using both open access medium-spatial resolution data and the application of commercially available high-resolution data. These data are used to determine risks for communities, and provide clear, understandable and non-specialist mapping to support organisations in their understanding of required response measures; particularly where potential exploitation risk in the longer-term following disaster events is more likely to occur. This paper outlines a post-hazard risk mapping effort to identify areas of concern in the context of The Bahamas using Hurricane Dorian as a case study, to explore and explain how such risk maps could be of benefit to a

Table 1

Details of the satellite sensor products that were used as part of the analysis to determine Hurricane Dorian impacts on The Bahamas.

Satellite	Sensor/Products	Corrections	Source	Imagery Dates	Spatial Resolution (m)	Spectral Bands
Sentinel-2	Orthorectified Optical (OLI) MSI Level-1C product	Top-of-atmosphere (TOA) radiometrically and geometrically corrected product	Copernicus Sci Hub (now Copernicus Data Space Ecosystem)	January 18, 2019 October 17, 2019 November 2, 2019	10	Band 3 – Green Band 4 – Red Band 5 – Red Edge Band 8 – NIR Band 12 – SWIR
Sentinel-1	Level 1C Band SAR Single Look Complex (SLC) product	Deburst, Orbital correction, Polarimetric Decomposition, Terrain Correction and Speckle filtering		March 2, 2019 September 2, 2019 September 4, 2019 September 7, 2019 January 8, 2020	20	VV and VH Polarization
	Level 1A Ground Range Detected (GRD) product	Radiometric correction, normalised backscatter generation and multi-looking		August 31, 2019 September 2, 2019 September 4, 2019	10	VV and VH Polarization
Planet Scope	4-band Ortho-tile	PlanetScope radiometric and sensor corrected product	Google Earth Engine (GEE)	Monthly averaged mosaic: September and March of 2018 2019, and 2020	3	Red Green Blue NIR

new audience beyond those traditionally in the humanitarian space – those working to support communities at risk of human trafficking in complex post-disaster contexts.

2. Data and methods

2.1. Data sources

Both optical (Sentinel-2, PlanetScope 4-band OrthoTile & Landsat-8) and radar (Sentinel-1) (Table 1) data were downloaded, pre-processed, analysed, and used to establish the extent of the impact of Hurricane Dorian on The Bahamas. Additionally, the study used data from Map Action (2019) to extract areas of infrastructure damage (a rasterized number of total buildings and percentage of buildings destroyed were processed). A variety of timescales were used in order to capture different trends; the primary data sources (Sentinel-1/2) had data aligned most closely with the hazard event (see Table 1), whereas those that were used for validation – the PlanetScope data – had a broader timeframe in order to provide validation from further outside of the period of Hurricane Dorian to determine the scope and scale of changes and validate them.

The Sentinel-2 data provided coverage for six islands of The Bahamas, and data with minimum cloud cover were sourced for the period immediately before and after Hurricane Dorian; including the imagery from the October 17, 2019 which was the earliest cloud-free image immediately post-disaster. The temporal resolution of Sentinel-2 (A and B) and Sentinel-1 (A) temporally is 5 days (combined constellation) and 10 days respectively, which provides a unique avenue to track changes caused by Hurricane Dorian using openly available data at low cost. This was supplemented by optical 3m spatial-resolution visible and near-infrared (VNIR) daily data from PlanetScope sensors. Monthly average mosaics for all islands across The Bahamas were downloaded. Cloud rates were filtered to 0–5% for the tiles that were to be analysed and mosaicked; due to the geographic and climatic conditions of the tropics, the threshold for inclusion of images with more than 5% cloud cover was raised as a trade-off for fuller coverage in some cases. Our analysis was restricted here due the limited spectral bands and radiometric noise of the imagery (Frazier and Hemingway, 2021; Valman et al., 2024). Whilst several new algorithms to undertake cloud-masking have been developed, they were unavailable on GEE where our analysis was completed (e.g. Wang et al., 2021). Sentinel-1C Band SAR data were used to generate dual polarization products to map areas impacted following Hurricane Dorian. Several scenes from the Single Look Complex (SLC) product covering the entire stretch of The Bahamas (in both ascending and descending orbit) were acquired (Fig. S2) and pre-processed (Ozigis et al., 2018) to generate alpha entropy decomposition image products. Further, Sentinel-1A Ground Range Detected (GDR) product was used to implement a backscatter analysis. These data were also pre-processed (see Ozigis et al., 2020) to obtain a full cross sectional backscatter layer of storm affected areas on Grand Bahama and Abaco. All Sentinel-2 optical bands and Sentinel-1 SAR products were resampled to a uniform spatial resolution of 10m using nearest neighbour, based on the WGS84 reference system. This was to ensure a uniform scale and representation of spatial features across multiple layers analysed for flood mapping and damage assessments in this study.

2.2. Analysis

2.2.1. Sentinel-2 and PlanetScope derived optical indices

For the analysis, three indices were calculated based on the tiles identified. Both NDVI and NDWI were calculated using the same methods applied to the Sentinel-2 data. Finally, SAVI was conducted for comparison with the Sentinel-2; however, the bands

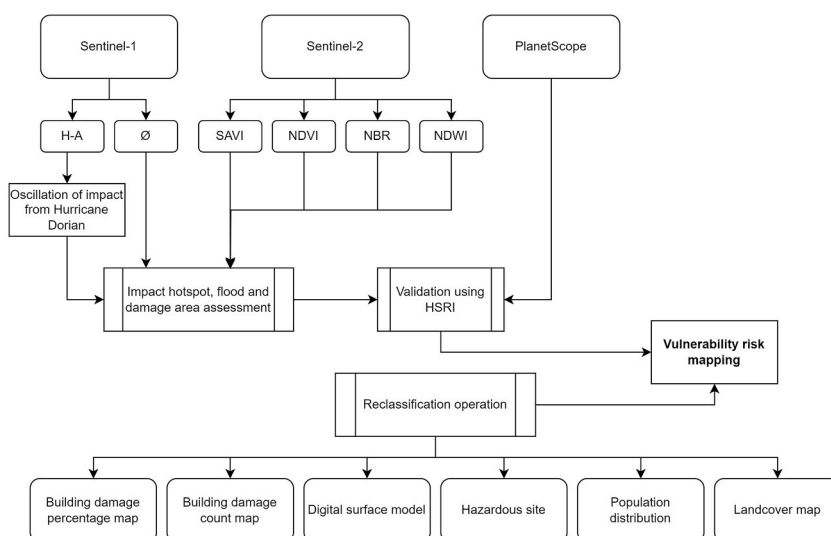


Fig. 1. Methodological flowchart for assessing overall risk through combined EO data.

commonly used in this analysis are not available in the 4-band PlanetScope data. Therefore, we applied the [Huete \(1988\)](#) method for SAVI for sensors with no shortwave-infrared (SWIR) bands ([Hoa, 2017](#)). NBR was not possible for PlanetScope data but was applied to Sentinel-2 sources. These indices were applied to understand the scale of impact from Hurricane Dorian and determine the environmental and potential socio-economic risks that communities across The Bahamas faced due to the disaster. We utilised the median values of the vegetation indices around affected areas pre- and post-disaster images in a trend analysis to further inform on the impact-recovery cycle of vegetation, which further validates the SAR analysis. Previous studies (see [Michener and Houhoulis, 1997](#); [Byun et al., 2015](#); [Priya and Vani, 2024](#)) have relied on similar approaches for disaster trend assessments. The assumption is that in the period prior to disaster vegetation greenness and health/vigour is usually high and intact. Immediately post-disaster the greenness generally reduces owing to flooding and canopy destruction; allowing more time post-disaster usually shows recovery and restoration of vegetation. The primary optical analysis was conducted using Sentinel-2 with validation provided through PlanetScope data ([Fig. 1](#)). These indices were applied to the five islands – Abaco, Grand Bahama, New Providence, Exuma and Eleuthera.

NDVI: The Normalised Difference Vegetation Index (NDVI; Eq. (1)) is used to infer vegetation growth, greenness and biomass abundance, and relies on the VNIR wavelengths to generate an indicator of health plant presence. NDVI is commonly used to establish the impact of hazards such as flooding, wildfire, and landslide ([Konda et al., 2018](#)).

$$NDVI = \frac{NIR - RED}{NIR + RED} \quad (1)$$

NDWI: The Normalised Difference Water Index (NDWI) is a widely used vegetation index due to its ability to depict moisture related stress in vegetation ([Gao, 1996](#)). NDWI is calculated using the NIR and SWIR bands, and widely applicable to detect and monitor vegetation conditions over large areas. As NDWI is influenced by both desiccation and wilting in the vegetation canopy, it is a more sensitive indicator than NDVI for drought monitoring. Eq. (2) was applied to Sentinel-2 data, whilst Eq. (3) was applied to the PlanetScope data due to the fewer available bands.

$$NDWI1 = \frac{NIR - SWIR}{NIR + SWIR} \quad (2)$$

$$NDWI^2 = \frac{GREEN - NIR}{GREEN + NIR} \quad (3)$$

NBR: The Normalised Burn Ratio (NBR; Eq. (4)) was used due to its ability to discreetly compare submerged vegetation and healthy vegetation. NBR primarily identifies burned areas and a measure of severity. It is calculated as a ratio between the NIR and SWIR values. This provides information on the vigour and moisture of vegetation by combining NIR and mid-infrared reflectance values ([Veraverbeke et al., 2010](#)).

$$NBR = \frac{NIR - SWIR}{NIR + SWIR} \quad (4)$$

SAVI: The Soil Adjusted Vegetation Index (SAVI; Eq. (5)) was generated and used to improve the true surface representation of The Bahamas, highlighting the extent of damage caused by Hurricane Dorian. The index offers a superior visualisation to NDVI as it corrects for the influence of soil brightness in areas where vegetative cover is low.

$$SAVI = \frac{NIR - RED}{NIR + RED + L} \times (1 + L) \quad (5)$$

2.2.2. Sentinel-1 derived radar indices

Backscatter Sigma 0: Following the Sentinel-1 GRD product pre-processing (radiometric and geometric corrections applied) the images were converted into a cross-sectional backscatter product (Eq. (6)). This converted the resultant images from Digital Number (DN) into Decibels (DB). The DB image is a logarithmic output with range values between +50 and –50 (depending on intensity) and represents more evenly distributed values over the panchromatic colour range, leading to less extreme values.

$$\delta DB = 10 \log 10 \delta \quad (6)$$

Alpha Angle: The Alpha Angle is one component derivative if the Alpha Entropy (H-A) decomposition, dual polarization (VV and VH) decomposition algorithm. The H-A Polarimetric decompositions reconcile and characterize the radar backscatter into a 2x2 coherency scattering matrix, before being expanded to the alpha classification plan to entropy, anisotropy and alpha planes ([Pottier and Lee, 2000](#)). The H-A decomposition method ([Cloude, 2007](#)) reconciled the three Sentinel-1 SLC products into three derivatives: entropy, anisotropy and alpha angle.

The entropy layer represents randomness in energy scattered, while the alpha (a) angle reconciles scattered energy into single, multiple, and volume scatter; the anisotropy layer estimates the importance of the secondary scattering phenomenon. When combined these variables provide an image enabling understanding of pre- and post-disaster change resulting from Hurricane Dorian. For this study, the alpha angle was used to make deductions on the extent of the impact of the storm on The Bahamas.

2.2.3. Hurricane Dorian impact mapping and damage hotspot assessment

Three Sentinel-1 images (before, immediately after, and several months after the storm) established the overall impact of Hurricane Dorian on the social-ecological landscape of The Bahamas. The generated alpha-entropy decomposition images – using a threshold

angle of 0.3–0.56 entropy and anisotropy (signifying moderate randomness) and alpha angle of greater than 65° (signifying areas with increased volume scattering) – were used to map the general impact of the hurricane across the islands of Abaco and Grand Bahama. The threshold presented the best values that helped to distinguish between static features in the period before the storm (pre-disaster images), and dynamic changes in features (post-disaster), especially in built-up areas. The threshold image highlighting impacted areas was reconciled and validated against ground reference data, high-resolution satellite images, and damage data.

The Sentinel-1 GRD pre-processed backscatter layers before and after Hurricane Dorian allowed the implementation of a targeted hotspot assessment of Abaco and Grand Bahama. This analysis focused on determining specific areas affected by the combined effect of flooding, landslide and extreme damage. Backscatter values across the VV and VH channels often ranged between –10 dB and 2 dB; however, to detect areas affected by flooding we used thresholds between –5 dB and –10 dB to cluster and identify areas affected that were validated by ground-data. The high influence of precipitation and moisture affected several thresholds, which caused misclassification among features.

2.2.4. Vulnerability to severe environmental and socio-economic risk mapping

The vulnerability mapping identified areas with particularly severe socio-economic and environmental impacts following Hurricane Dorian and served as a guide for tracking future ‘at-risk’ areas. Several risk factor maps (Table 2) were identified based on previous hurricane assessments (Ogundipe et al., 2018), acquired, and pre-processed into a standardised raster layer before integration via weighted sum overlay to generate the final vulnerability risk map.

The polarity of the raster layers was realigned to assume a uniform direction of low values (e.g., zero representing low vulnerability/risk and 10 for high risk/vulnerability); this technique integrates raster layers using a common measurement scale and weighs each input layer according to its given importance. For this study, equal weights were assigned to the seven input rasters. The assignment of equal weight reduced bias in the final vulnerability map. The risk analysis was implemented (Fig. 1) to establish areas that were, and could be, susceptible to the most severe environmental, social and economic impact of hazards to the scale of a hurricane.

3. Results

3.1. Sentinel-2 derived indices

From the indices analysis, the NBR presented the most dynamic and sinusoidal trend of change from minimum to maximum values on Abaco (Fig. 2), detecting clear impacts caused by the hurricane aligned with the storm path. The median NBR was 0.7 (pre-), 0.3 (during-), and 0.6 (post-disaster) showing more bare ground in the period where Hurricane Dorian hit. The same analyses were also undertaken for the island of Grand Bahama. For this island, the results also suggest that the NBR – but also the SAVI (which becomes saturated less quickly and enables clearer assessment) – showed expected dynamic trends of change between pre- and post-disaster to identify significantly affected areas of damage caused by Hurricane Dorian (Fig. 3). For Grand Bahama, the median NBR values in this case were 0.7, 0.3, and 0.8 over the course of the analysis period. Both outcomes suggests that in the period prior to Hurricane Dorian, vegetation cover are largely intact, and greenness is usually high, before reducing because of the storm and beginning recovery (with greater recovery in vegetation in Grand Bahamas compared to Abaco). Other indices (in this case NDVI and NDWI) presented less variability in median values over the assessment timeframe across the two most heavily impacted islands (but the NDVI were validated by PlanetScope data; see Figs. S3 and S4). Changes in the NDVI (observed changes in a range of 0.2–0.4) showed substantial decline in the during-hurricane imagery owing to the destruction of branches, stems and leaves. However, several months post-disaster, results showed that vegetation (from these indices) have recovered in certain areas, leading to a concomitant increase in NDVI values.

For islands that received less direct impact from Hurricane Dorian there were other general trends observed (Figs. S5–7). On New Providence – site of the capital, Nassau – SAVI provided the best and expected variability in median values (of 0.6 pre-, 0.2 during-, and 0.5 post-disaster), with dips in the immediate aftermath of Hurricane Dorian indicating bare soil – or in this case the presence of bare tree canopies and trunks; before recovery to almost pre-hurricane indices measurements, again suggesting a clearing and then recovery of vegetation across the lesser impacted islands. However, cloud-cover restricted the analysis and deductions of affected coastal regions; despite this the areas where coverage was available were sufficient to reach conclusions on the viability of the indices. The optical vegetation health indices for the islands of Exuma and Eleuthera resulted in little to no variation across the analysis period suggesting minimal impact to the landscape and communities. This is likely due to the distance of the islands (300 km) from the path of the storm (Avila et al., 2020) combined with relatively small landmasses (Exuma is 250 km² and Eleuthera is 457 km²).

Table 2

Details of vulnerability mapping overlays combining environmental and socio-economic layers for risks mapping.

Layer	Source
Digital Surface Model	Advanced Land Observatory Satellite Phased Array Land Synthetic Aperture Radar (ALOS PALSAR)
Flood Inundated Areas	Sentinel – GRD (primary analysis from this study (Figs. 5 and 6 for Grand Bahama and Abaco)
Building Damage Count Map	Map Action
Building Damage Percentage Map	Map Action
Hazardous Site Map	Map Action
Population GRID Data	WorldPop
Land Cover Data	Environmental System Research Institute (ESRI) LULC Product 2022

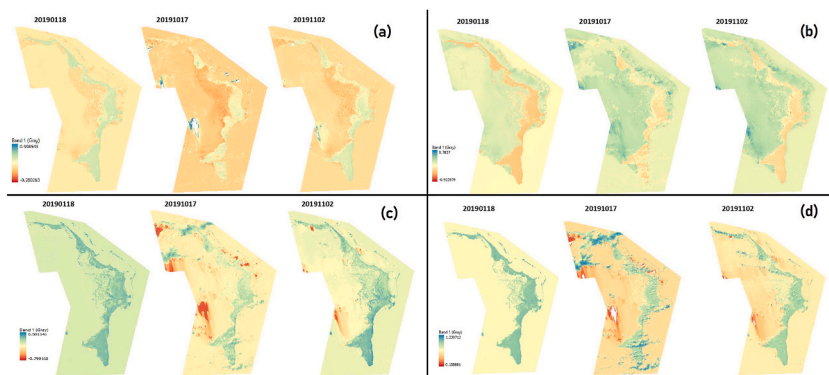


Fig. 2. Derived vegetation health indices for Abaco showing from left to right in each version the pre-disaster, during-disaster, and post-disaster results for: (a) NDVI, (b) NDWI, (c) NBR, and (d) SAVI.

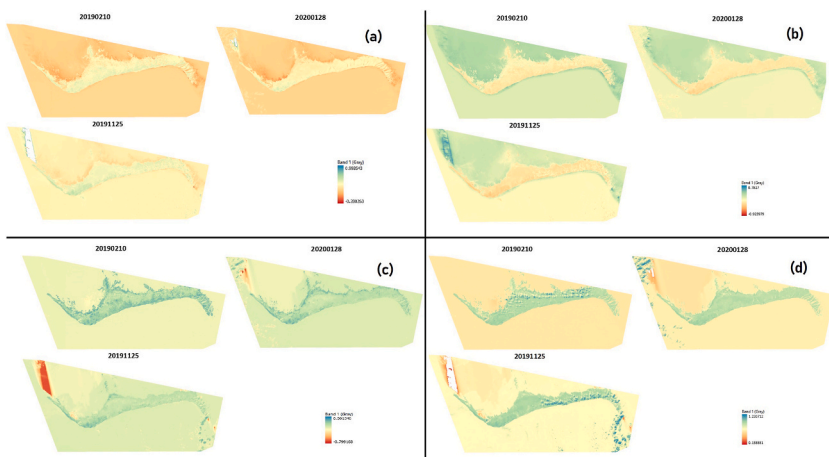


Fig. 3. Derived vegetation health indices for Grand Bahama showing from left to right in each version the pre-disaster, during-disaster, and post-disaster results for: (a) NDVI, (b) NDWI, (c) NBR, and (d) SAVI.

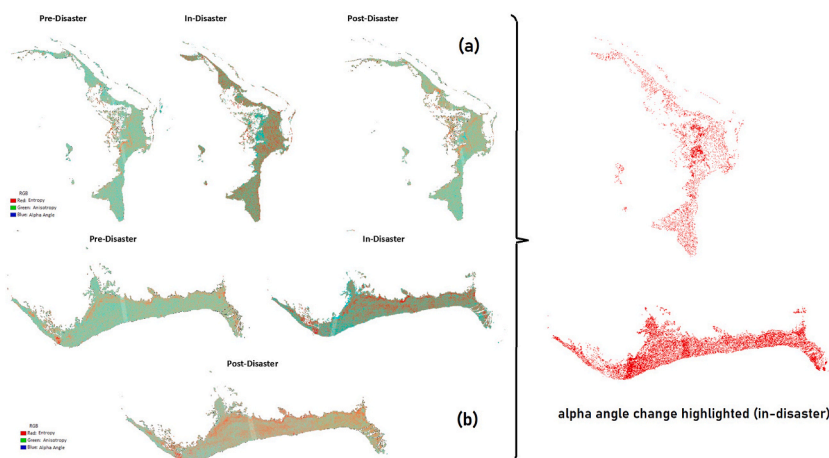


Fig. 4. Alpha entropy decomposition derived from Sentinel-1 SAR data for main islands (a) Abaco and (b) Grand Bahama impacted before, during and after Hurricane Dorian. The threshold outputs from the alpha angle are also highlighted on the right of the image, showing areas of significant change (during-disaster) in the immediate period following the storm.

3.2. Sentinel-1 derived alpha-entropy decomposition

The results from the derived alpha and entropy decomposition (Fig. 4) show consistent changes and variability in the pre- and post-disaster data potentially linked to the effects of Hurricane Dorian. For Abaco the H-A output indicates a higher influence of alpha angle and randomness from anisotropy potentially due to flooding in the period immediately following the storm (i.e., the during-disaster image). In addition, entropy (right-hand side Fig. 4) increased for all during-disaster imagery across all five analysed islands (New Providence, Exuma, and Eleuthera are shown in Fig. S6). This reflects trends seen in previous post-hurricane analyses across the Caribbean (Ogundipe et al., 2018) and is likely linked to the loss of tree cover during the storm meaning less SAR scattering overall.

For the islands that experienced less direct impacts, similar trends were observed (see Fig. S8) and are consistent with the observed spectral changes from the Sentinel-2 derived NBR. Grand Bahama showed a strong protraction of anisotropy in the post-disaster imagery, with the spatial extent representing significant levels of backscatter alteration indicating impact from the hurricane.

The thresholding operation on the alpha angle layer from H-A (Fig. 4) highlights areas of significant change. This analysis shows promise in identifying areas of change, with Grand Bahama showing clear alignment with the changes reported in Fig. 4. Similar trends are visible in the three islands with lesser storm impact (Fig. S8). The threshold operation provided better representation of areas likely affected by flood impact, damage to the vegetation canopy, landslides, and building damage – highlighting locations where

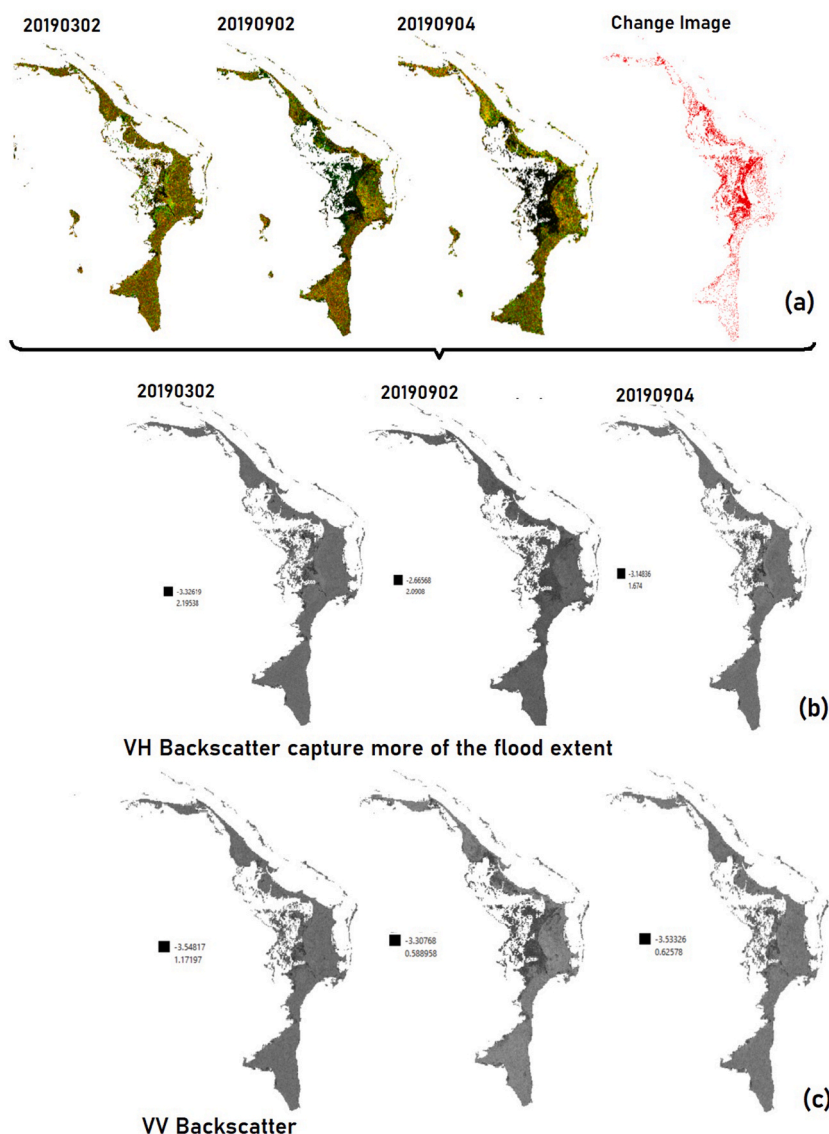


Fig. 5. Sentinel-1 SAR Backscatter for Abaco showing comparison and detected damage hotspot areas. (a) VV-VH Composite for the period before and after Hurricane Dorian, as well as the flooded areas in the change imagery; (b) shows the VH Backscatter both before and after the storm, and (c) shows the VV Backscatter alone for the period before and after the storm which were used to generate the composite analysis images shown in (a).

displacement and community vulnerability are more likely to occur. These changes owe to the observed change in anisotropy (random scattering) caused by the volume scatter of the target surface in the post-disaster imagery from November 2019 (Table 1).

3.3. Damage hotspot assessment

The damage hotspot analysis (based on Sentinel-1 derived backscatter data) showed large areas of Abaco and Grand Bahama were affected by flooding (Fig. 5), particularly in coastal areas. The data analysed from the September 2, 2019 and September 4, 2019 in Fig. 5a captures the true spatial extent of flooding during the hurricane; this was not present prior to the storm and had subsided in 2020 data. In total, an area of around 25 km² was submerged by the flooding according to our findings, with critical infrastructure including the airport, service lines, agricultural land, and housing affected.

Similarly, almost 40 km² of coastal land, beaches, and near-shore land was submerged because of Hurricane Dorian on Grand Bahama (Fig. 6a). However, the findings from the backscatter analysis suggest this could be higher in the immediate period following the storm (September 4, 2019); as large dark patches are observed in the central mangrove-dominated areas of the island (which align with ground-data gathered in April 2023).

3.4. Combined risk mapping

Results from the weighted overlay of critical factor maps (based on data from Table 2) for the two main affected islands of Abaco (Fig. 7) and Grand Bahama (Fig. 8) highlight key areas where Hurricane Dorian impacted populations. For the former, the most central parts of the islands are at risk of substantial flooding and physical damage to infrastructure, properties, and communities due to the low-lying landscape. The most secure area (and less susceptible to flooding) areas on Abaco were areas of higher elevation where larger settlements and most of the reported official population were based. Similar patterns were noted for Grand Bahama as many low-lying areas (again central to the island) were susceptible to flooding during the storm, and the concomitant physical damage which follows a hurricane event (e.g., damaged buildings, forest loss).

3.5. Validation

Due to the impact of the Covid-19 pandemic, on-site verification was not possible until April 2023. Despite this, signs of the hurricane impact were still visible. Extensive areas with bare tree trunks were observed, caused by the winds stripping away branches and leaves (Fig. 9a). Fires also occurred during the disaster and were seen in the presence of burnt tree trunks, resulting from forest fires (McKenzie et al., 2023). Re-growth is beginning to occur with grass and small plants growing amongst the damaged trees at ground-level. This provides validation to the NDVI changes observed in Fig. 2 with the pre-, during- and post-disaster NDVI results showing a decrease in the immediate period following Dorian making landfall, followed by a slight increase some months afterwards. These trends were observed on both Grand Bahama and Abaco – although seen to a greater extent in the latter as the island bore the first direct impact. Our ground-referencing also provided evidence that saturated ground from even small amounts of rainfall caused localised flooding (Fig. 9b), particularly in the areas where some of the most economically insecure communities reside, exacerbating long-term recovery opportunities.

4. Discussion

EO has a clear role in the tracking of impacts following disasters to support the delivery of humanitarian assistance. Designs for novel post-disaster aid distribution methods have previously been developed using data produced by this study (see Ogundipe and

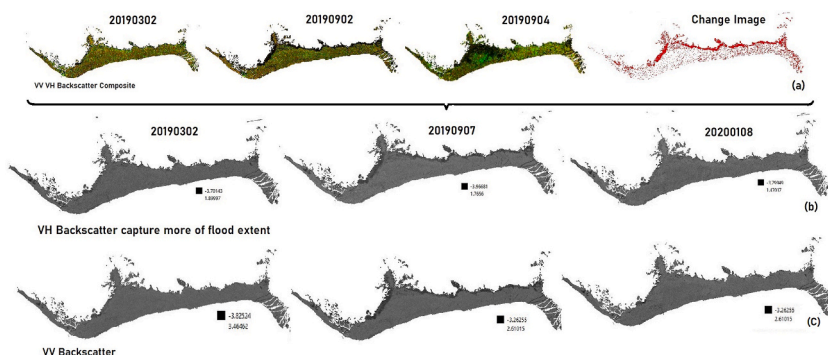


Fig. 6. Sentinel-1 SAR Backscatter for Grand Bahama showing comparison and detected damage hotspot areas. (a) VV-VH Composite for the period before and after Hurricane Dorian, as well as the flooded areas in the change imagery; (b) shows the VH Backscatter both before and after the storm, and (c) shows the VV Backscatter alone for the period before and after the storm which were used to generate the composite analysis images shown in (a).

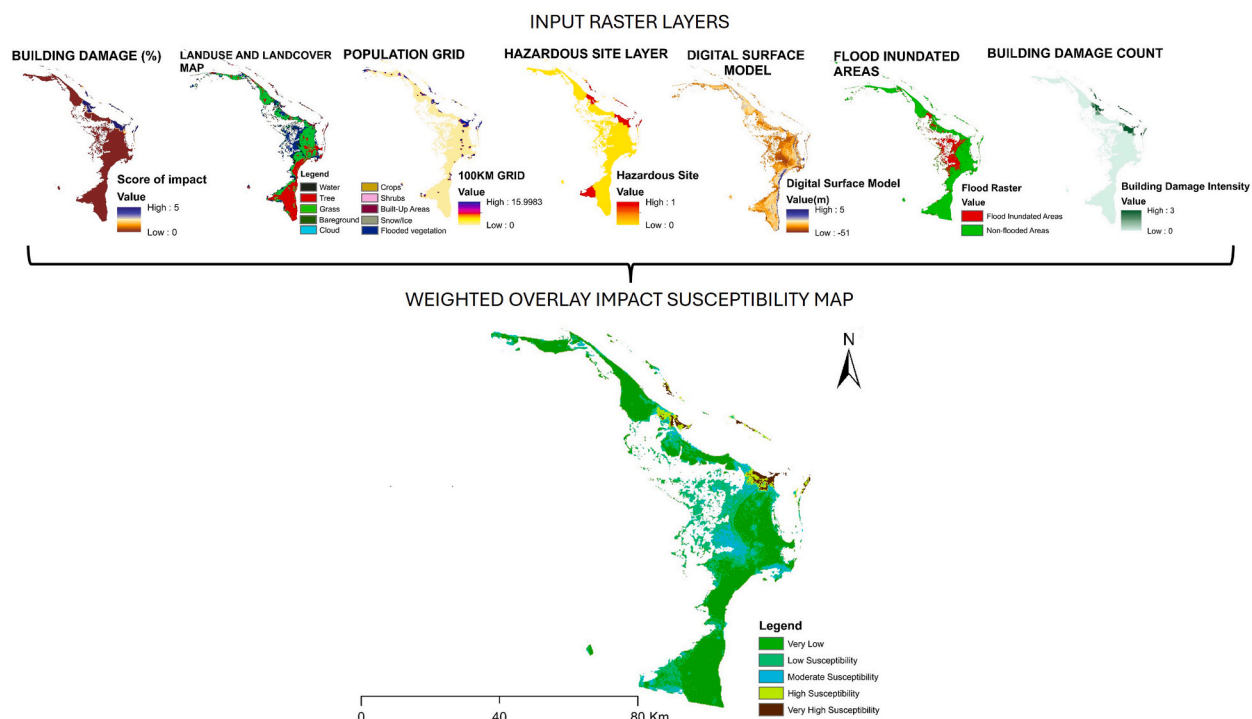


Fig. 7. Integrated Risk Map for Great Abaco showing the levels of risk and vulnerability to severe damages in several parts of the islands. Areas highlighted in red colour suggest high susceptibility to severe environmental and socio-economic impacts (especially in the central Abaco area), while areas in green colour suggest low susceptibility to socio-economic impacts as they are largely uninhabited.

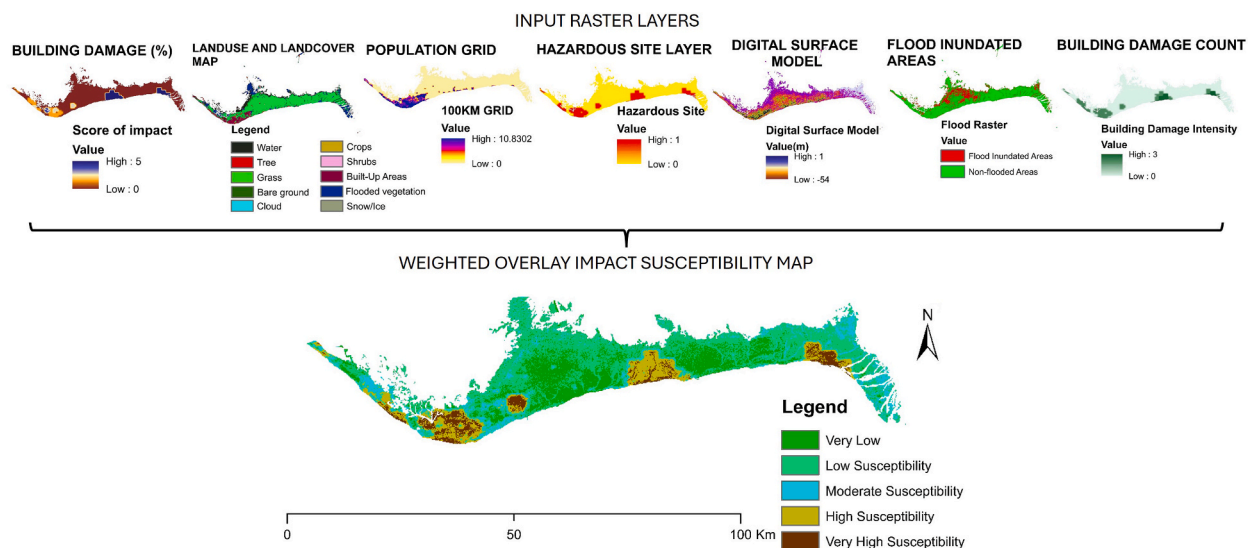


Fig. 8. Integrated Risk Map for Grand Bahama Island showing the levels of risk and vulnerability to severe damages in several parts of the islands. Areas highlighted in red colour suggest high susceptibility to severe environmental and socio-economic impacts (especially in the Freeport area), while areas in green colour suggest low susceptibility to socio-economic impacts as they are largely uninhabited (including areas in the Central hinterlands).

Jackson, 2023). Tracking change over the duration of a disaster via EO is a vital component of humanitarian response, further supporting exposure mapping, adaptation planning and preparedness, and response activities (Le Cozannet et al., 2020; Sousa et al., 2021). Monitoring long-term recovery should be integrated into recovery efforts and ensuring communities are able to access support. This includes using EO as an advocacy tool for gaining support for communities who continue to face the effects of disasters and



Fig. 9. Images from ground-reference data collected in The Bahamas from April 2023; (a) shows the remains of tree cover from a forest damaged on Abaco, and (b) shows localised flooding in the aftermath of brief heavy rains whilst on Grand Bahama.

climate change impacts – for example, Haitian migrant communities who were adversely affected by Hurricane Dorian (Behm, 2019). Such long-term monitoring has previously been implemented to understand the natural recovery rates in the Southern United States following Hurricane Katrina, as well as tracking the need for indices development to better mitigate against the impacts of hurricanes in the future (Li et al., 2016).

Technological innovations in EO could improve temporal monitoring. This study faced barriers to data collection including the effects of the pandemic preventing ground-reference data collection closer to Hurricane Dorian, and the scale of data – both in volume and size – also led to long period of data-processing. Advancements across the EO sector in the last decade are now enabling improvements that will enhance real-time response and faster-processing speeds for events in the future. For example, smallsat constellations - with their high spatial coverage, low cost, and ability to repeat-capture data on a single location over short-time scales - provide an economically efficient method for response and management during disaster events (Santilli et al., 2018). One example is the PlanetLabs Crisis Response Programme (PlanetLabs, 2024a), which utilises data, such as those we have used in our study, to support organisations involved in disaster response to gain insights through select imagery relevant to the response from the Planet constellation of around 200 satellites (PlanetLabs, 2024b). These targeted provisions of data from smallsat constellations build on the principles held by large-scale government and commercial providers of satellite data pioneered through the [International Charter Space and Major Disasters \(2024a\)](#) protocol - including data sharing and targeted acquisitions. The charter was activated on September 4, 2019 in response to Hurricane Dorian as requested by The Bahamas National Emergency Management Administration (NEMA), providing data on multiple issues including flooding and damage assessments ([International Charter Space and Major Disasters, 2024b](#)).

Many of the applications of EO in disaster response however do not truly capture the social vulnerability that can follow hazard exposure, which our analysis seeks to correct. Some of the most marginalised communities in this instance, the Haitian migrant populations, often resided in informal yet long-established settlements known as The Mudd and the Peas, which were decimated by the hurricane (Behm, 2019; Rolle, 2019). Concerns for marginalised Haitian populations and further exposure to socio-economic vulnerabilities following community displacement is something that could be supported through ongoing EO. This tool could be powerful in targeting resource dissemination, improved infrastructure and social programming by community organisations. Yet it should be used with caution when considering governmental engagement as a significant shift in the political discourse is required to move away from their present anti-Haitian agenda; as such these technologies could pose an additional risk of harm if used incorrectly adding to the discrimination already faced. Risks of exploitation of highly vulnerable communities following disasters could be challenged through prevention activities following timely risk mapping monitoring. For example, the populations of the Mudd and the Peas experienced storm surge inundation (Fig. 5) (Rolle, 2019); meaning that those surviving the hurricane suffered the loss of homes, documentation and livelihoods as well as exposure to physical safety risks and deportation. Such precarity has been noted in other rapid-onset hazard events as being an integral part of the connection between environmental factors and the exploitation of communities (Bharadwaj et al., 2021; Decker Sparks et al., 2021; O'Connell, 2021). Compounding risk factors are reflected in the pressure placed on agricultural land (noted in Figs. 7 and 8) and can lead to further economic pressures which have a 'multiplier' effect upon already vulnerable populations. The damage to the small agricultural sector, affecting food security, may exacerbate economic risks as The Bahamas rely on imported goods (US Department of Commerce, 2024), further placing economic burdens on impacted populations. Such compounding risks can lead to increased vulnerabilities which may lead to exploitation and human trafficking risks as people attempt to rebuild and recover from disasters like Hurricane Dorian. The application of EO to investigate issues of labour exploitation have previously been identified (see Jackson et al., 2018) and their applications have been demonstrated in other geographic and environmental contexts (Boyd et al., 2021; Koukoulou et al., 2021; Brown et al., 2022). Combining the lens of social support for recovery and prevention of additional harms is something that the rapid EO responses mentioned above through real-time monitoring and risk mapping can support.

There were several limitations within the application of the satellite data, particularly those associated with the PlanetScope sensors. For example, direct comparative analysis for indices were not available in all cases due to the limited number of bands within

the sensor. Application of the SAVI indices required the use of different bands compared with the Sentinel-2 MSI sensor, which limits the direct comparative assessments that can be made. Further, the bands from the PlanetScope sensor are limited to the extent that the NBR analysis could not be undertaken using these data, and an alternative methodology could not be sourced at the time of the data processing, reducing the capacity of high-spatial resolution indices that were available within the study. Moreover, to mitigate some of the limitations to optical data usage – which can be challenging during periods of high-cloud cover such as storms – we utilised a combination of data sources, most notably using SAR products and multiple data sources in tandem to generate the combined risk map. In future research, the application of Sentinel-1 data via a Dual-Polarized Water Index (SDWI) (Li et al., 2023) could be used to assess risks in real time during a hurricane as SAR enables assessment under conditions of heavy cloud cover. Perhaps the largest issue, was the ability to undertake validation via ground-based data sources, as the research team were unable to travel to The Bahamas until 3.5 years after Hurricane Dorian. To tackle this, we used a combination of data from fieldwork (April 2023) and PlanetScope data to address some of these concerns. Unfortunately, due to the time and funding constraints of the research, additional validation sources were unable to be secured.

Whilst threshold analysis has provided good results in this post-disaster case study in The Bahamas, advancements in the integration and application of artificial intelligence (AI) could support real-time risk mapping assessments in response to disasters (Al Shafian and Hu, 2024). These methods can enhance and build upon the example risk assessments in this study. AI has the potential to improve the speed and accessibility of response, enabling socially oriented support which may limit additional crises such as human trafficking. These approaches may ensure that EO data are more effective and ensure timelier implementation of all economic, social, health, and environmentally focused responses through the improvement of hazard monitoring (Ivić, 2019; Kim and Kim, 2020; Zhu and Ye, 2022; Cao, 2023; Akhyar et al., 2024). Daily monitoring is also being explored. For example, PlanetScope imagery using AI methods have shown promise in daily river monitoring (Valman et al., 2024) and such applications could be adapted for flood mapping during hazard events. Using PlanetScope to build robust monitoring systems to cope with future disaster events would benefit from further cloud-masking algorithms (e.g., Wang et al., 2021) to work on GEE and overcome the radiometric quality shortcomings and insufficient default quality masks of the PlanetScope data at present (Wang et al., 2021; Frazier and Hemingway, 2021; Valman et al., 2024). The speed and ability to process high volumes of data using AI would also mitigate against some of the limitations of our own study. In our validation data from PlanetScope we generated a monthly mosaic to mitigate against cloud-cover issues, yet some of the nuance and characteristics that may present themselves in fluctuating daily changes may have been missed through the stitching and mosaicking processes; including those key dates during the storm period where cloud coverage was high. By combining optical analysis with SAR from Sentinel-1 different patterns could be identified. But real-time observations identified at speed through AI risk mapping models could provide such data at a rate in-line with the event when combined with constellations providing disaster response support. As such, any response to the physical impacts of a hazard, and related social risks (including issues such as human trafficking and labour exploitation) need to use a combination of satellite sensor data sources at speed through AI applications.

As climate change continues to influence global hazards (Reed et al., 2022), the humanitarian response community must continue to incorporate human rights framings and their links to climate change into Disaster Risk Response (DRR) planning and frameworks. EO risk mapping can aid in the planning and prevention stages of DRRs as well as the immediate implementation of responses; it is in the former where a human rights focus can provide benefits (Shucksmith, 2017a) including for vulnerable communities in times of disaster. Mandating and providing protections to communities experiencing disasters is vital for the security (economic, social, health, and environmental) of communities (Shucksmith, 2017b) and as such should be incorporated into planning and delivering support to impacted populations. Furthermore, organisations seeking to support and address vulnerable populations should be aware that the intersecting risks of hazards and the impacts that follow (e.g., displacement, economic losses) (Stout, 2018; Bales, 2021) can lead to increased risks for potentially already vulnerable populations and expansion of disaster risk mapping should be shared amongst communities seeking to support such populations in order to reduce the likelihood of additional harms, including human trafficking.

5. Conclusion

EO has a vast role to play in the monitoring of risks following hurricanes – to both respond and prepare for future vulnerabilities among communities likely to face exposure to more extreme climatic events and risks of social and economic exploitation. Risk mapping in real-time should be oriented to focus on a human rights-based approach and incorporate community preparedness (pre-disaster), responses (during and immediately post-disaster), and targeted recovery support (post-disaster) that can limit community vulnerability. Our study focused on understanding the role that EO can play in responding to Hurricane Dorian in The Bahamas highlighting the need for real-time and focused support for ensuring marginalised communities who are often the most impacted receive the support they require by those who are seeking to help them (e.g., community organisation). EO alone cannot be the only activity, but as a tool it has repeatedly demonstrated its vital role in hazard preparation and response; increasing its role to include social responses to prevent additional socio-economic pressure in disaster responses should also be prioritised.

CRedit authorship contribution statement

Mohammed Ozigis: Writing – review & editing, Writing – original draft, Visualization, Formal analysis, Data curation. **Oluropo Ogundipe:** Writing – review & editing, Writing – original draft, Visualization, Validation, Supervision, Methodology, Funding acquisition, Formal analysis, Data curation, Conceptualization. **Samuel J. Valman:** Writing – review & editing, Visualization, Validation, Methodology, Formal analysis, Data curation. **Jessica L. Decker Sparks:** Writing – review & editing, Supervision, Project administration, Funding acquisition, Conceptualization. **Helen McCabe:** Writing – review & editing, Funding acquisition,

Conceptualization. **Rebekah Yore:** Writing – review & editing, Funding acquisition, Conceptualization. **Bethany Jackson:** Writing – review & editing, Writing – original draft, Visualization, Supervision, Project administration, Formal analysis, Data curation.

Ethics Statement

Ethical Approval for the project was granted by the Research Ethics Committee in the School of Geography, University of Nottingham. No interaction with human subjects was included in this part of the study. All relevant ethical guidelines were followed.

Funding

This work was supported by the Templeton World Charity Foundation (TWCF) [grant number 5466695; amendments 15714776, 19993277] provided to the Rights Lab, University of Nottingham.

Declaration of competing interest

The authors declare the following financial interests/personal relationships which may be considered as potential competing interests:

Bethany Jackson reports financial support was provided by Templeton World Charity Foundation Inc. If there are other authors, they declare that they have no known competing financial interests or personal relationships that could have appeared to influence the work reported in this paper.

Acknowledgements

The authors would like to thank those in The Bahamas who were gracious in sharing their experiences with the research team across the duration of the project; and Prof. Doreen Boyd for providing access to the PlanetScope data through an active PlanetLabs data licence.

Appendix A. Supplementary data

Supplementary data to this article can be found online at <https://doi.org/10.1016/j.rsase.2025.101466>.

Data availability

<https://github.com/SamValman/EOHurricaneDorian>

References

- Akhyar, A., Zulkifley, M.A., Lee, J., Song, T., Han, J., Cho, C., Hyun, S., Son, Y., Hong, B.-W., 2024. Deep artificial intelligence applications for natural disaster management systems: a methodological review. *Ecol. Indicat.* 163, 112067.
- Al Shafian, S., Hu, D., 2024. Integrating machine learning and remote sensing in disaster management: a decadal review of post-disaster building damage assessment. *Buildings* 14 (8), 2344.
- Avila, L.A., Stewart, S.R., Berg, R., Hagen, A.B., 2020. Hurricane dorian. National Hurricane Center Tropical Cyclone Report. NOAA, Washington DC.
- Bales, K., 2021. What is the link between natural disasters and human trafficking and slavery? *Journal of Modern Slavery* 6 (3), 34–45.
- Behm, M., 2019. Abaco's dark clouds: five months after hurricane dorian, Haitian immigrants struggle to find shelter and schools. WUFT News. Retrieved 14 July, 2023. <https://projects.wuft.org/keline-five-months-after-hurricane-dorian-there-is-still-struggle/>.
- Bennett, M.M., Smith, L.C., 2017. Advances in using multitemporal night-time lights satellite imagery to detect, estimate, and monitor socioeconomic dynamics. *Rem. Sens. Environ.* 192, 176–197.
- Bethell-Bennett, I., Rolle, S.A., Minnis, J., Adderley, E.D., 2022. The economic and social impact of hurricane dorian and covid-19 on tourism in selected islands in the Bahamas. In: Bethell-Bennett, I., Rolle, S.A., Minnis, J., Okumus, F. (Eds.), *Pandemics, Disasters, Sustainability, Tourism: an Examination of Impact on and Resilience in Caribbean Small Island Developing States*. Emerald Insight, Bingley.
- Bharadwaj, R., Bishop, D., Hazra, S., Pufaa, E., Kofi Annan, J., 2021. Climate-induced Migration and Modern Slavery: a Toolkit for Policymakers. IIED, London.
- Blumenstock, J.E., 2016. Fighting poverty with data. *Science* 353 (6301), 753–754.
- Boccardo, P., Tonolo, F.G., 2015. Remote sensing role in emergency mapping for disaster response. In: Lollino, G., Manconi, A., Guzzetti, F., Culshaw, M., Bobrowsky, P., Luino, F. (Eds.), *Engineering Geology for Society and Territory: Urban Geology, Sustainable Planning and Landscape Exploitation*, ume 5. Springer, International, Switzerland.
- Boyd, D.S., Jackson, B., Wardlaw, J., Foody, G.M., Marsh, S., Bales, K., 2018. Slavery from space: demonstrating the role for satellite remote sensing to inform evidence-based action related to UN SDG number 8. *ISPRS J. Photogrammetry Remote Sens.* 142, 380–388.
- Boyd, D.S., Perrat, B., Li, X., Jackson, B., Landman, T., Ling, F., Bales, K., Choi-Fitzpatrick, A., Goulding, J., Marsh, S., Foody, G.M., 2021. Informing action for United Nations SDG target 8.7 and interdependent SDGs: examining modern slavery from space. *Humanities and Social Sciences Communications* 8 (1), 111.
- Brown, C., Boyd, D.S., Kara, S., 2022. Landscape analysis of cobalt mining activities from 2009 to 2021 using very high resolution satellite data (democratic republic of the Congo). *Sustainability* 14 (15), 9545.
- Brown, C., Daniels, A., Boyd, D.S., Sowter, A., Foody, G.M., Kara, S., 2020. Investigating the potential of radar interferometry for monitoring rural artisanal cobalt mines in the Democratic Republic of the Congo. *Sustainability* 12 (23), 9834.
- Byun, Y., Han, Y., Chae, T., 2015. Image fusion-based change detection for flood extent extraction using bi-temporal very high-resolution satellite images. *Rem. Sens.* 7 (8), 10347–10363.

- Cao, L., 2023. AI and data science for smart emergency, crisis and disaster resilience. *International Journal of Data Science and Analytics* 15, 231–246.
- Cerrai, D., Yang, Q., Shen, X., Koukoulou, M., Anagnostou, E.N., 2020. Brief communication: hurricane Dorian: automated near-real-time mapping of the “unprecedented” flooding in the Bahamas using synthetic aperture radar. *Nat. Hazards Earth Syst. Sci.* 20, 1463–1468.
- Cheng, C.-S., Behzadan, A.H., Noshadran, A., 2021. Deep learning for post-hurricane aerial damage assessment of buildings. *Comput. Aided Civ. Infrastruct. Eng.* 36, 695–710.
- Cloude, S., 2007. The dual polarization entropy/alpha decomposition: a PALSAR case study. *Science and Applications of SAR Polarimetry and Polarimetric Interferometry* 644, 2.
- Coelho, S., 2016. The Climate Change-Human Trafficking Nexus. IOM, Bangkok.
- de Beurs, K.M., McThompson, N.S., Owsley, B.C., Henebry, G.M., 2019. Hurricane damage detection on four major Caribbean islands. *Rem. Sens. Environ.* 229, 1–13.
- Decker Sparks, J.L., Boyd, D.S., Jackson, B., Ives, C.D., Bales, K., 2021. Growing evidence of the interconnections between modern slavery, environmental degradation, and climate change. *One Earth* 4 (2), 181–191.
- Deng, L., Wang, Y., 2022. Post-disaster building damage assessment based on improved U-Net. *Sci. Rep.* 12, 15862.
- Elvidge, C.D., Baugh, K.E., Anderson, S.J., Sutton, P.C., Ghosh, T., 2012. The Night Light Development Index (NLDI): a spatially explicit measure of human development from satellite data. *Soc. Geogr.* 7, 23–35.
- Foody, G.M., Ling, F., Boyd, D.S., Li, X., Wardlaw, J., 2019. Earth observation and machine learning to meet sustainable development goal 8.7: mapping sites associated with slavery from space. *Rem. Sens.* 11 (3), 266.
- Frazier, A.E., Hemingway, B.L., 2021. A technical review of Planet smallsat data: practical considerations for processing and using PlanetScope imagery. *Rem. Sens.* 13 (19), 3930.
- Gao, B.-C., 1996. NdwI – a normalized difference water index for remote sensing of vegetation liquid water from space. *Rem. Sens. Environ.* 58 (3), 257–266.
- Ghaffarian, S., Farhadabad, A.R., Kerle, N., 2020. Post-disaster recovery monitoring with google Earth engine. *Appl. Sci.* 10 (13), 4574.
- Greenal, S., Anilkumar, S., 2024. Development of digital support tools for post-disaster infrastructure reconstruction and recovery: a scoping study. *Sustainable and Resilient Infrastructure*. <https://doi.org/10.1080/23789689.2024.2365502>.
- Hargreaves, P.K., Watmough, G.R., 2020. Satellite Earth observation of socioeconomic conditions for improved poverty reporting. In: *Proceedings of SPIE 11527 Space, Satellites, and Sustainability*, 1152708.
- Head, A., Manguin, M., Tran, N., Blumenstock, J.E., 2017. Can human development be measured with satellite imagery? *Proceedings of ICTD 16–19. November, Lahore*.
- Hoa, N.H., 2017. Comparison of various spectral indices for estimating mangrove covers using PlanetScope data: a case study in Xuan Thuy National Park, Nam Dinh Province. *Management of Forest Resources and Environment* 5, 74–83.
- Hoque, M.A.-A., Phinn, S., Roelfsema, C., Childs, I., 2017. Tropical cyclone disaster management using remote sensing and spatial analysis: a review. *Int. J. Disaster Risk Reduc.* 22, 345–354.
- Huete, A.R., 1988. A soil-adjusted vegetation index (SAVI). *Rem. Sens. Environ.* 25 (3), 295–309.
- IFRC, 2023. Final report the Bahamas: hurricane dorian. International Federation of Red Cross and Red Crescent Societies, Nassau.
- Inter-American Development Bank (IDB), 2020. Assessment of the effects and impacts of hurricane dorian in the Bahamas. ECLAC. LC/TS.2020/31.
- International Charter Space and Major Disasters, 2024a. About the charter. Retrieved 10 June 2024, from. <https://disasterscharter.org/web/guest/about-the-charter>.
- International Charter Space and Major Disasters, 2024b. Charter activations: hurricane dorian in Bahamas. Retrieved 10 June 2024, from. <https://disasterscharter.org/web/guest/activations/-/article/storm-hurricane-urban-in-bahamas-activation-620>.
- Ivić, M., 2019. Artificial intelligence and geospatial analysis in disaster management. *Int. Arch. Photogram. Rem. Sens. Spatial Inf. Sci.* XLII-3/W8.
- Jackson, B., Bales, K., Owen, S., Wardlaw, J., Boyd, D.S., 2018. Analysing slavery through satellite technology: how remote sensing could revolutionise data collection to help end modern slavery. *Journal of Modern Slavery* 4 (2), 169–199.
- Jackson, B., Boyd, D.S., Ives, C.D., Decker Sparks, J.L., Foody, G.M., Marsh, S., Bales, K., 2020b. Remote sensing of fish-processing in the Sundarbans Reserve Forest, Bangladesh: an insight into the modern slavery-environment nexus in the coastal fringe. *Maritime Studies* 19, 429–444.
- Jackson, B., Decker Sparks, J.L., Brown, C., Boyd, D.S., 2020a. Understanding the co-occurrence of tree loss and modern slavery to improve efficacy of conservation actions and policies. *Conservation Science and Practice* 2 (5), e183.
- Karaer, A., Ulak, M.B., Abichou, T., Arghandeh, R., Ozguven, E.E., 2021. Post-hurricane vegetative debris assessment using spectral indices derived from satellite imagery. *Transport. Res. Rec.* 2675 (12), 504–523.
- Kim, J., Kim, D.-j., 2020. Satellite imagery and AI-based disaster monitoring and establishing a feasible integrated near real-time disaster monitoring system. *Journal of the Korean Association of Geographic Information Studies* 23 (3), 236–251.
- Konda, V.G.R.K., Chejarla, V.R., Mandla, V.R., Voleti, V., Chokkavarapu, N., 2018. Vegetation damage assessment due to Hudhud cyclone based on NDVI using Landsat-8 satellite imagery. *Arabian J. Geosci.* 11, 1–11.
- Koukoulou, I., Cakir, M.S., Kunz, N., Boyd, D.S., Trautrim, A., Hatzinikolaou, K., Gold, S., 2021. A multi-method approach to prioritize locations of labor exploitation for ground-based interventions. *Prod. Oper. Manag.* 30 (12), 4396–4411.
- Le Cozannet, G., Kervyn, M., Russo, S., Ifejika Speranza, C., Ferrier, P., Fomelis, M., Lopez, T., Modaresi, H., 2020. Space-based Earth observations for disaster risk management. *Surv. Geophys.* 41, 1209–1235.
- Li, X., Yu, L., Xu, Y., Yang, J., Gong, P., 2016. Ten years after Hurricane Katrina: monitoring recovery in New Orleans and the surrounding areas using remote sensing. *Sci. Bull.* 61, 1460–1470.
- Li, H., Xu, Z., Zhou, Y., He, X., He, M., 2023. Flood monitoring using sentinel-1 SAR for agricultural disaster assessment in poyang lake region. *Rem. Sens.* 15 (21), 5247.
- Map Action, 2019. Building damage count and building damage percentage map. Retrieved 5 July 2024, from. https://maps.mapaction.org/dataset?_license_id_limit=0&res=format=PDF&vocab=&groups=2019-bhs-001&vocab_product_themes=Situation+and+Damage&page=2.
- Marazita, J., 2020. Displacement in paradise: hurricane dorian slams the Bahamas: thematic report. Internal Displacement Monitoring Centre (IDMC), Geneva.
- Marlier, M.E., Resetar, S.A., Lachman, B.E., Anania, K., Adams, K., 2022. Remote sensing for natural disaster recovery: lessons learned from Hurricanes Irma and Maria in Puerto Rico. *Environ. Sci. Pol.* 132, 153–159.
- McKenzie, Z., Kumler, M.P., Ma, R., Williams, K., Hayes, W.K., 2023. Eyes from the sky: application of satellite-based indices to assess vegetation casualty on Grand Bahama Island one-year post-Hurricane Dorian. *Remote Sens. Appl.: Society and Environment* 32, 101044.
- Michener, W.K., Houhoulis, P.F., 1997. Detection of vegetation changes associated with extensive flooding in a forested system. *Photogramm. Eng. Rem. Sens.* 63 (12), 1363–1374.
- Nhamo, G., Chikodzi, D., 2021. Use and contestations of Earth observation technologies in disaster risk reduction and management. In: Nhamo, G., Chikodzi, D. (Eds.), *Cyclones in Southern Africa. Volume 1: Interfacing the Catastrophic Impact of Cyclone Idai with SDGs in Zimbabwe. Sustainable Development Goal Series*. Springer Nature, Switzerland.
- O’Connell, C., 2021. From a Vicious to a Virtuous Circle: Addressing Climate Change, Environmental Destruction and Contemporary Slavery. *Anti-Slavery International*, London.
- Ogundipe, O., Jackson, B., 2023. Foresight DRM: disaster mapping hackathon. Retrieved 10 June 2024, from. <https://www.nottingham.ac.uk/research/beacons-of-excellence/rights-lab/resources/reports-and-briefings/2023/may/foresight-drm-disaster-mapping-hackathon.pdf>.
- Ogundipe, O., Ozigis, M.S., Beazer, S., 2018. The use of satellite data to assess the impact of recent hurricanes on agriculture in the caribbean. Presented at the Caribbean Week of Agriculture, 8-12 October 2018, Barbados.
- Ozigis, M.S., Kaduk, J., Jarvis, C., Ogochukwu, A., 2018. Assessment of terrestrial oil spill dynamics using field spectra and Sentinel 1 H- α decomposition. In: *Sixth International Conference on Remote Sensing and Geoinformation of the Environment (RSCy2018) SPIE*, vol. 10773, pp. 117–125.
- Ozigis, M.S., Kaduk, J.D., Jarvis, C., da Conceição Bispo, P., Balzter, H., 2020. Detection of oil pollution impacts on vegetation using multifrequency SAR, multispectral images with fuzzy forest and random forest methods. *Environ. Pollut.* 256, 113360.

- Patz, J., 2005. Satellite remote sensing can improve chances of achieving sustainable health. *Environ. Health Perspect.* 113 (2), A84–A85.
- Percival, G.S., Alameh, N.S., Caumont, H., Moe, K.L., Evans, J.D., 2013. Improving disaster management using Earth observations–GEOSS and CEOS activities. *IEEE J. Sel. Top. Appl. Earth Obs. Rem. Sens.* 6 (3), 1368–1375.
- PlanetLabs, 2024a. Disaster data. Retrieved 10 June 2024, from. <https://www.planet.com/disasterdata/>.
- PlanetLabs, 2024b. Planet FAQ: how many satellites does Planet have in orbit? Retrieved 10 June 2024, from. <https://www.planet.com/faqs>.
- Pottier, E., Lee, J.S., 2000. Application of the «H/A/alpha» polarimetric decomposition theorem for unsupervised classification of fully polarimetric SAR data based on the Wishart distribution. *SAR Workshop: CEOS Committee on Earth Observation Satellites* 450, 335.
- Priya, R.S., Vani, K., 2024. Vegetation change detection and recovery assessment based on post-fire satellite imagery using deep learning. *Sci. Rep.* 14, 12611.
- Reed, K.A., Wehner, M.F., Zarzycki, C.M., 2022. Attribution of 2020 hurricane season extreme rainfall to human-induced climate change. *Nat. Commun.* 13, 1905.
- Rolle, R., 2019. How the Mudd and pigeon Peas were lost. *The Tribune*. Retrieved 5 July, 2024, from. <https://www.tribune242.com/news/2019/sep/07/how-mudd-and-pigeon-peas-were-lost/>.
- Sadiq, R., Akhtar, X., Imran, M., Ofli, F., 2022. Integrating remote sensing and social sensing for flood mapping. *Remote Sens. Appl.: Society and Environment* 25, 100697.
- Santilli, G., Vendittozzi, C., Cappelletti, C., Battistini, S., Gessini, P., 2018. CubeSat constellations for disaster management in remote areas. *Acta Astronaut.* 145, 11–17.
- Schultz, J.M., Sands, D.E., Kossin, J.P., Galea, S., 2020. Double environmental injustice - climate change, Hurricane Dorian, and the Bahamas. *N. Engl. J. Med.* 382, 1–3.
- Shucksmith, C., 2017a. Methods to incorporate human rights law into disaster prevention and reduction strategies. *Blog of the European Journal of International Law*. Retrieved 12 June 2024, from. <https://www.ejiltalk.org/methods-to-incorporate-human-rights-law-into-disaster-prevention-and-reduction-strategies/>.
- Shucksmith, C., 2017b. Building human security through humanitarian protection and assistance: the potential of the international committee of the red cross. *J. Confl. Transform. Secur.* 6 (1), 56–78.
- Smith, D., 2019. 'The poor are punished': Dorian lays bare inequality in the Bahamas. *Guardian* from. <https://www.theguardian.com/world/2019/sep/13/hurricane-dorian-the-mudd-haitians-inequality>. (Accessed 14 July 2023).
- Sorek-Hamer, M., Just, A.C., Kloog, I., 2016. Satellite remote sensing in epidemiological studies. *Curr. Opin. Pediatr.* 28 (2), 228–234.
- Sousa, J.J., Liu, G., Fan, J., Perski, Z., Steger, S., Bai, S., Wei, L., Salvi, S., Wang, Q., Tu, J., Tong, L., Mayrhofer, P., Sonnenschein, R., Liu, S., Mao, Y., Tolomei, C., Bignami, C., Atzori, S., Pezzo, G., Wu, L., Yan, S., Peres, E., 2021. Geohazards monitoring and assessment using multi-source Earth observation techniques. *Rem. Sens.* 13 (21), 4269.
- Stout, S., 2018. Human Trafficking in the Wake of Natural Disasters: Is the United States Any Different than Third World Countries? University of Arkansas, Fayetteville.
- Stryker, T., Jones, B., 2009. Disaster Response and the International Charter Program. *Photogrammetric Engineering & Remote Sensing*, pp. 1342–1344.
- Thomas, A., Benjamin, L., 2022. Climate justice and loss and damage: hurricane Dorian, Haitians and human rights. *Geogr. J.* 1–9. <https://doi.org/10.1111/geoj.12484>.
- Tralli, D.M., Blom, R.G., Zlotnicki, V., Donnellan, A., Evans, D.L., 2005. Satellite remote sensing of earthquake, flood, landslide and coastal inundation hazards. *ISPRS J. Photogrammetry Remote Sens.* 59 (4), 185–198.
- US Department of Commerce, 2024. Bahamas country commercial guide – agricultural sectors. Retrieved 5 July, 2024, from. <https://www.trade.gov/country-commercial-guides/bahamas-agricultural-sectors>.
- USAID, 1991. Remote sensing in natural hazard assessments. In: *Primer on Natural Hazard Management in Integrated Regional Development Planning*. Department of Regional Development and Environment Executive Secretariat for Economic and Social Affairs Organization of American States, Washington DC. <https://www.oas.org/dsd/publications/unit/oea66e/begin.htm#Contents>.
- Valman, S.J., Boyd, D.S., Carboneau, P.E., Johnson, M.F., Dugdale, S.J., 2024. An AI approach to operationalise global daily PlanetScope satellite imagery for river water masking. *Rem. Sens. Environ.* 301, 113932.
- Veraverbeke, S., Lhermitte, S., Verstraeten, W.W., Goossens, R., 2010. The temporal dimension of differenced Normalized Burn Ratio (dNBR) fire/burn severity studies: the case of the large 2007 Peloponnese wildfires in Greece. *Rem. Sens. Environ.* 114 (11), 2548–2563.
- Voigt, S., Kemper, T., Riedlinger, T., Kiefl, R., Scholte, K., Mehl, H., 2007. Satellite image analysis for disaster and crisis-management support. *IEEE Trans. Geosci. Rem. Sens.* 45 (6), 1520–1528.
- Vongsantivanich, W., Holvoet, N., Chaimatanan, S., Delahaye, D., 2018. Mission planning for a non-homogenous Earth observation satellite constellation for disaster response. In: *AIAA SpaceOps Conference*, 28 May–1 June, Marseille.
- Wang, J., Yang, D., Chen, S., Zhu, X., Wu, S., Bogonovich, M., Guo, Z., Zhu, Z., Wu, J., 2021. Automatic cloud and cloud shadow detection in tropical areas for PlanetScope satellite images. *Rem. Sens. Environ.* 264, 112604.
- Watmough, G.R., Atkinson, P.M., Hutton, C.W., 2013. Predicting socioeconomic conditions from satellite sensor data in rural developing countries: a case study using female literacy in Assam, India. *Appl. Geogr.* 44, 192–200.
- Zegarra, M.A., Alvarez, L.G., Gartner, M., Palomino, L., 2021. The Macro-Economic Effects of Hurricanes in the Bahamas: A Case Study Using Satellite Night Light Luminosity. *Inter-American Development Bank. Caribbean*.
- Zegarra, M.A., Schmid, J.P., Palomino, L., Seminario, B., 2020. Impact of hurricane dorian in the Bahamas: a view from the sky. *Inter-American Development Bank (IDB), Country Department Caribbean Group*, Nassau.
- Zhu, Z., Ye, S., 2022. These AI and Satellite Mapping Techniques Are Speeding up the Process of Disaster Management. *World Economic Forum*. Retrieved 10 June 2024, from. <https://www.weforum.org/agenda/2022/10/new-satellite-mapping-with-ai-can-quickly-pinpoint-hurricane-damage-across-an-entire-state-to-spot-where-people-may-be-trapped/>.